nature geoscience

LETTERS

PUBLISHED ONLINE: 26 SEPTEMBER 2010 | DOI: 10.1038/NGEO967

Stress transfer between thirteen successive dyke intrusions in Ethiopia

Ian J. Hamling[1]*†, Tim J. Wright[1], Eric Calais[2], Laura Bennati[2] and Elias Lewi[3]

Stress transfer from a large earthquake may trigger subsequent earthquakes in nearby regions[1–3]. Such a mechanism has been suggested for a few isolated cases of magmatic intrusions and eruptions[4–6], but has not been systematically demonstrated. An ongoing rifting episode, which began in 2005, along the Nubia–Arabia plate boundary provides a unique opportunity to test any such linkage. The intrusion of a 60-km-long magmatic dyke marked the beginning of the episode[7–12] and, between June 2006 and July 2009, 12 more dykes were emplaced[13]. Here we use geodetic surveys and simple dislocation models to locate and quantify the extension that occurred during each event. We identify regions where tensile stress was increased (unclamped) by the previous dyke intrusions. Of the 12 events that followed the initial intrusion, nine dykes were observed to have at least half of their opening in regions unclamped by the previous events. We propose that the transfer of stress links the 13 dyke intrusion events. We suggest that the stress change that is induced by a new dyke is an important factor in determining the location of future events and could help improve volcanic hazard analysis.

In September 2005, the 60-km-long Dabbahu rift segment[14], within the sub-aerial arm of the Red Sea Rift (Fig. 1b), ruptured in Northern Afar, Ethiopia, marking the beginning of a continuing rifting episode[7–12,15,16]. Since the initial ~2.5 km^3 dyke intrusion, a further 12 discrete dykes have been detected along the Dabbahu rift segment, injecting an additional ~1 km^3 of new material. Interferometric synthetic aperture radar (InSAR, and seismicity data indicate that the 2005 dyke was fed from shallow chambers beneath two volcanoes at the northern end of the segment, Dabbahu and Gabho, and a deeper reservoir at Ado'Ale near the segment centre[7,12]. Subsequent dyke intrusions emplaced between June 2006 and July 2009 have all been fed from Ado'Ale[13,16,17]. Here we investigate whether the location of new dyke intrusions, emplaced between June 2006 and July 2009, can be explained by the stress changes induced by previous activity. The unusually large number of magmatic intrusions allows us, for the first time, to reach a definitive conclusion on the role of stress transfer in magmatic intrusions.

Following the method described in Hamling *et al.*[13], we use elastic dislocation models to calculate the stress change caused by each new dyke intrusion. The models are a result of the inversion of InSAR and, where available, GPS data to find the best fitting opening distribution on a dyke plane in an elastic half space[18] (Methods). We allow opening to occur down to a depth of 20 km. The majority of the intrusions are located in the upper 10–15 km; opening below ~10 km is small relative to the main intrusion and is, in general, a result of the inversion fitting long wavelength signals not related to the dyke opening. Therefore, before we calculate the change in stress we discard areas where the opening is smaller than the local $2-\sigma$ uncertainty (typically ~0.3–0.4 m). The resultant opening models (Fig. 2) are then used to compute the internal strain and stress fields. The dyke model is discretized into 1,500 1 km by 1 km patches and the change in stress is calculated at the centre of each patch (Fig. 1a). We calculate the stress perpendicular to the local dyke plane by rotating the stress tensor[19] (see Methods for more details). The resultant normal stresses from each intrusion are plotted on the dyke plane (Fig. 2), with compressive stress changes (clamping) defined as negative and tensile stress changes (unclamping) as positive.

Although the initial state of stress along the rift segment is unknown before the onset of rifting in 2005, we can test whether the spatial pattern of magmatic intrusion during the recent activity can be explained by the transfer of stress after each new event. If this is the case we would expect new dyking to occur preferentially in areas of unclamping[5].

The September 2005 dyke ruptured the length of the Dabbahu rift segment. All of the dykes intruded since 2006 have been emplaced along the same rift segment in a section where the amount of opening in the September 2005 dyke was lower. To assess whether stress transfer is important in controlling the location of the next event we examine the percentage of dyke opening occurring in regions of positive stress change. We set a lower threshold of 0.1 MPa (1 bar) to ensure that relatively small stress changes do not bias the result. For the first intrusion, emplaced in June 2006, we find that 45% of the opening is in sections unclamped by the September 2005 event. The next intrusion, had 91% of its opening in regions unclamped by the previous intrusion (Fig. 2) and ~89% of the third dyke occurred in areas unclamped by the second intrusion (Supplementary Table S1, Fig. 2).

Dykes 4, 5 and 6 follow a similar pattern with 95, 58 and 80% of their respective openings occurring in regions unclamped by the previous intrusion (Fig. 2). Dyke 7 had 56% of its opening in regions of unclamping caused by the previous intrusion with dykes 8 and 9 having 78 and 100% of their openings in unclamped sections of the rift. Interestingly the eighth intrusion initially appeared to reintrude the same area as the previous dyke; however, the inversion revealed that it was intruded directly beneath dyke 7 (Fig. 2). The final three intrusions of the sequence jump northward. Dyke 10 was located to the north of Ado'Ale, ~5 km from the previous dyke and with only 4% of the opening occurring in regions of tensile stress generated by the previous intrusion. Dykes 11 and 12 migrate southwards with 35 and 86% of their openings in sections unclamped by the previous dykes respectively (Fig. 2).

To test whether the observed correlation between tensile stress and dyke location could have occurred by chance, we calculate the probability of randomly-positioned dykes of the same size having

[1]School of Earth and Environment, University of Leeds, Leeds LS2 9JT, UK, [2]Department of Earth and Atmospheric Sciences, Purdue University, Indiana 47907-1397, USA, [3]Institute of Geophysics Space Science and Astronomy, Addis Ababa University, Addis Ababa, P.O. Box 1176, Ethiopia. †Present address: Earth System Physics, ICTP (UNESCO-IAEA), Strada Costiera 11, 34151 Trieste, Italy. *e-mail: ihamling@ictp.it.

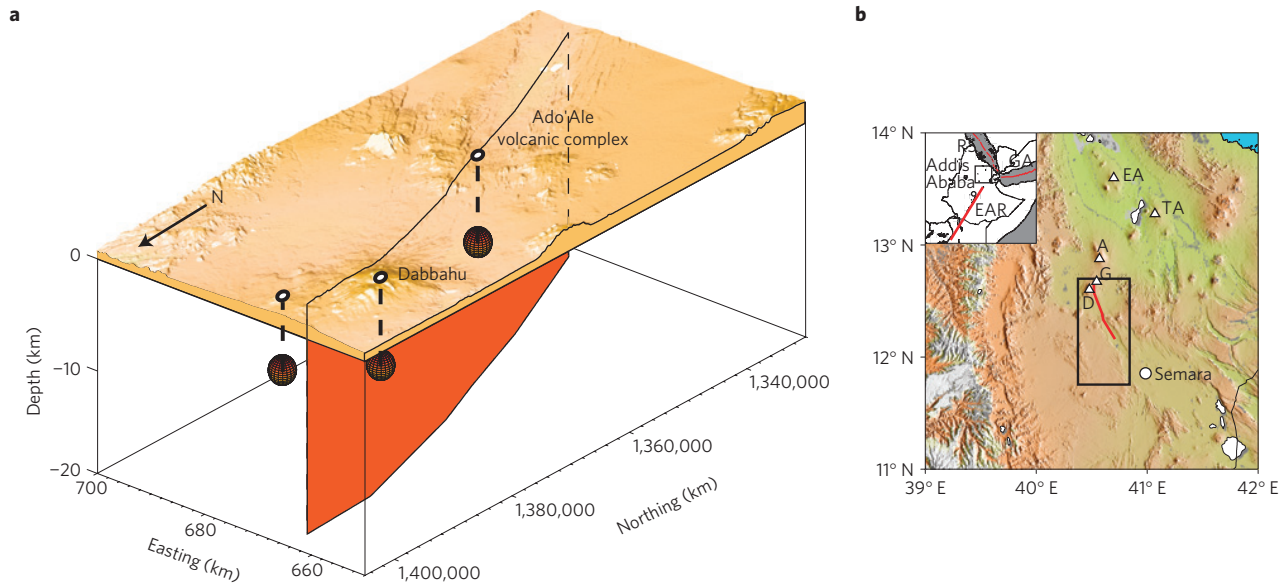

Figure 1 | Model geometry used for this study and colour shaded relief map of northern Afar and the study area. a, 3D projection of the modelled dyke plane beneath the Dabbahu rift segment. The rectangular region shows the location of the dyke along the rift segment, the orange spheres represent point source magma chambers at 5 km depth beneath Gabho and Dabbahu and at 8 km beneath Ado'Ale. **b**, Colour shaded relief map of northern Afar showing the location of the dyke (red line) intruded in 2005, Gabho (G), Dabbahu (D), Alayta (A), Ado'Ale (A'A), Tat'Ale (TA) and Erta'Ale (EA) volcanoes (white triangles) and Semara, the regional capital (white circle). The black box indicates the region shown in **b**.

the same (or higher) degree of opening in tensile regions. For each dyke, we calculate the percentage of opening that would be observed to occur in tensile regions for every possible location of the dyke along the whole model dyke plane. We then weight the likelihood of the dyke occurring at that location using a probability function derived from the observed locations of the real intrusions, which are more frequent near Ado'Ale (see Methods, Supplementary Fig. SM3). From this, we produce cumulative histograms that show the probability of each dyke exceeding a given tensile opening percentage (Fig. 3).

During the Dabbahu rifting episode, the mean percentage of opening in unclamped sections of the rift has been 70%, with seven of 12 dykes having over 75% of their opening in regions unclamped by the previous intrusion. The probabilities for individual dykes occurring in areas with the same amount of unclamping ranges from 0.06 to 0.78 (Fig. 3), with a mean of 0.4. The cumulative probability for the entire sequence of dykes occurring in regions with the observed amount of opening in unclamped regions is therefore vanishingly small (1 in 2 million). The amount of opening in unclamped sections of the rift for four events (5, 7, 10 and 11) was lower than the average, and ranged from 4 to 58%. Dyke 10 had over twice the average volume and a maximum opening of ~3 m, but only 4% of its opening was in an area significantly unclamped by dyke 9. The dyke was the most northerly of all the intrusions and was largely emplaced in a region which had not yet been reintruded by the post 2005 dykes. As such, if we consider the cumulative stress change caused by the dyking events since June 2006, then ~55% of the opening is in areas of tensile stress change. For dyke 11, only ~35% of its modelled opening occurred in sections unclamped by the previous intrusion, and its location suggests that it re-intruded the southern section of dyke 10 (Fig. 2). The magma source for all of the new dyke injections is located at Ado'Ale, indicating that this event must have propagated northward towards a region of high tensile stress induced by the previous dyke. This is not surprising; numerical simulations of the Krafla rifting episode in Iceland, between 1975 and 1984, suggest that dykes will preferentially propagate into regions of higher tensile stress[20], which would explain this northward migration. The modelled opening for the October intrusion extends to a depth of ~14 km into a zone of high conductivity, imaged using magnetotelluric (MT) methods[21], which may have prevented the dyke from cooling between the two intrusions, thus allowing it to be re-intruded.

It is well established that static stress changes, generated by earthquakes, influence the location and timing of subsequent events[1–3,22]; however, there are few studies which have examined the role of stress transfer in magma emplacement[4,5]. Amelung *et al.*[5] showed that magma intrusion between 2002 and 2005 at Mauna Loa was focused into regions of the rift segment unclamped by earlier events. Similarly, the dominant control on the location of the new dyking along the Dabbahu segment appears to be related to the stress change caused by the 2005 intrusion, with the majority of new magmatism occurring in regions of low opening during the 2005 event (Fig. 2). Furthermore, our results suggest that the dominant control in the location of the intrusions emplaced between June 2006 and July 2009 is the stress change caused by the previous intrusion rather than the cumulative stress of all the preceding intrusions. If we consider only the previous intrusion then the average amount of opening in regions of unclamping is ~70%. Considering the cumulative stress from the preceding two intrusions reduces the average to ~50%, and for the previous three intrusions to ~43%. Interestingly, the area surrounding the source region, inferred to be in the centre of the segment at between 8 and 10 km, is always in an area of tensile stress, which would enable magma to accumulate before it is intruded into adjacent regions of unclamping. It should be noted that we do not consider the effects of buoyancy forces or magma pressure. These effects have been shown to play an important role in magma intrusion and suggest that the final location of magmatic emplacement is a trade-off between the external stress field and internal pressure[20,23]. However, this study suggests that knowledge of the local stress changes induced by each new intrusion is sufficient to guide future magmatic events.

There are a number of other factors that may influence the location of new magmatism that we do not consider in these simple models. First, we do not consider the evolution of pressure of the magma source which ultimately drives each of the intrusions. The fact that the spatial distribution of magma over this period can be

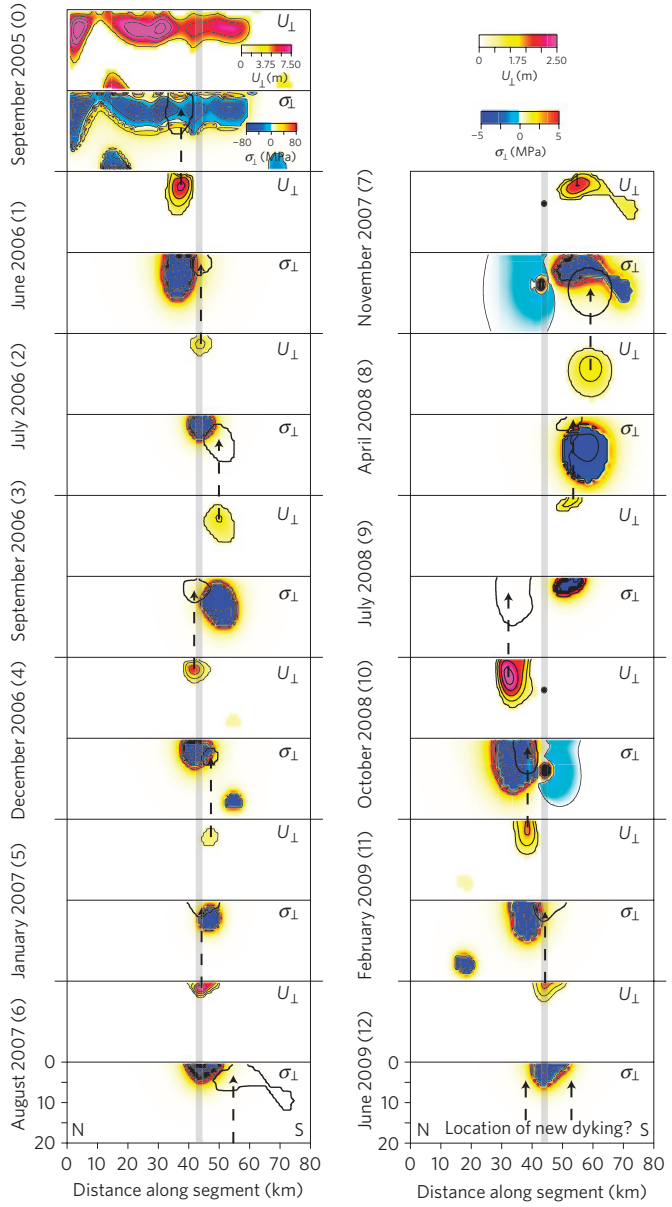

Figure 2 | Distributed opening models and stress change calculated for each of the dyke intrusions between September 2005 and June 2009. The top and bottom panels for each intrusion show the opening model and stress change respectively. The arrows and black outlines link the maximum opening of dyke N to the stress change induced by dyke $N-1$, and black circles represent deflating point sources for the intrusions in November 2007 and October 2008. All of the inversions assume a value of 32 GPa for both λ and μ. The grey solid line shows the location of Ado'Ale. $\sigma_\perp$ and $U_\perp$ are the stress change and opening perpendicular to the dyke plane respectively.

explained by the stress transfer from each dyke may suggest that there has been no significant change in magma pressure over the intrusion period. Also, we do not consider the stress change caused by the inflation of the magma source beneath the centre of the segment. However, the stress change induced by the inflating source is negligible compared with that caused by any of the new dykes. Also, we do not consider any relaxation of stresses after any of the dyke intrusions. However, Nooner *et al.*[24] have shown that 95% of the relaxation signal observed is related to the September 2005 dyke intrusion rather than the recent dyke intrusions, suggesting that this will have minimal affect on the stress change result.

Despite these simplifications, our results show that magma emplaced during the ongoing Dabbahu rifting episode is focused into regions of unclamping induced by previous dyking. This result indicates that the stress change, induced by a new dyke, is a controlling factor on the location of future events and should therefore be incorporated into routine volcanic hazard monitoring.

Methods

All of the interferograms used in this study were constructed using ASAR images from ESA's Envisat satellite and processed using JPL/Caltech ROI PAC software[25] (Supplementary Fig. S1). The topographic phase was removed using a 3 arcsecond 90 m resolution digital elevation model (DEM) generated by the NASA Shuttle radar topography mission (SRTM; ref. 26) and a power spectrum filter was applied[27]. Interferograms were unwrapped using the branch-cut method[28], with errors fixed manually. In addition to the InSAR data, continuously recording GPS data from up to 11 sites, installed in and around the rift segment in response to the 2005 dyke injection, were available covering some of the dyke intrusion events (Supplementary Fig. S2).

To invert for the opening distributions shown in Fig. 2, the InSAR data were first subsampled using a Quadtree algorithm. Each dyke was modelled as a rectangular dislocation in an elastic half-space, after the formulations of ref. 29. Using a downhill simplex inversion a set of parameters were found, which minimized the square misfit between model predictions and observations. The result of the inversion provides constraints on the geometry of the dyke plane (Fig. 1). With the geometry fixed, we perform a joint inversion of ascending and descending InSAR and GPS data to find the best-fitting distributed opening model, $\mathbf{m}$:

$$\begin{pmatrix} \mathbf{A}_{asc} & \mathbf{x} & \mathbf{y} & 1 & 0 & 0 & 0 & 0 & 0 & 0 \\ \mathbf{A}_{dsc} & 0 & 0 & 0 & \mathbf{x} & \mathbf{y} & 1 & 0 & 0 & 0 \\ \mathbf{A}_{gpsx} & 0 & 0 & 0 & 0 & 0 & 0 & 1 & 0 & 0 \\ \mathbf{A}_{gpsy} & 0 & 0 & 0 & 0 & 0 & 0 & 0 & 1 & 0 \\ \mathbf{A}_{gpsz} & 0 & 0 & 0 & 0 & 0 & 0 & 0 & 0 & 1 \\ \kappa\nabla^2 & 0 & 0 & 0 & 0 & 0 & 0 & 0 & 0 & 0 \end{pmatrix} \begin{pmatrix} \mathbf{m} \\ a_{asc} \\ b_{asc} \\ c_{asc} \\ a_{dsc} \\ b_{dsc} \\ c_{dsc} \\ c_{gpsx} \\ c_{gpsy} \\ c_{gpsz} \end{pmatrix} = \begin{pmatrix} \mathbf{d}_{asc} \\ \mathbf{d}_{dsc} \\ \mathbf{d}_{gpsx} \\ \mathbf{d}_{gpsy} \\ \mathbf{d}_{gpsz} \\ 0 \end{pmatrix}$$

where $\mathbf{A}_{asc}, \mathbf{A}_{dsc}, \mathbf{A}_{gpsx}, \mathbf{A}_{gpsy}$ and $\mathbf{A}_{gpsz}$ are a set of matrices representing Green's functions for the ascending and descending interferograms, GPS displacements in the x, y and z directions which, multiplied by $\mathbf{m}$ produce the model displacements at the observation points, $\mathbf{x}$ and $\mathbf{y}$, using the elastic dislocation formulation of Ref. 29; ∇^2 is the finite difference approximation of the Laplacian operator, which acts to smooth the distribution of slip and opening, the relative importance of which is governed by the size of the scalar smoothing factor κ; a and b are phase gradients in the x- and y-directions respectively; c are offsets to account for the unknown zero phase level (InSAR) or displacements at the reference GPS station (subscripts indicate data source); and $\mathbf{d}$ is a vector containing the observed displacements[13,30].

After solving for the opening distribution the internal stress field is then calculated by evaluating the following equations[18]:

$$\epsilon_{ij} = \frac{1}{2}\left(\frac{\partial u_i}{\partial x_j} + \frac{\partial u_j}{\partial x_i}\right)$$

$$\sigma_{ij} = \lambda\epsilon_{kk}\delta_{ij} + 2\mu\epsilon_{ij}$$

where ϵ and σ are the strain and stress, $\partial u/\partial x$ is the rate of change of displacement, λ and μ are Lame's constants and δ is the Kronecker delta. To determine the tensile stress perpendicular to the plane of the dyke, the stress tensor must first be rotated. Ref. 19 showed that the traction vector, $\mathbf{t}$, at a point on any surface can be defined, using indicial notation, by

$$\mathbf{t}_i(n) = \sigma_{\mathbf{ji}}\hat{\mathbf{n}}_\mathbf{j}$$

where $\hat{\mathbf{n}}$ is the outward normal vector. Expressed in matrix notation, in Cartesian co-ordinates, this becomes

$$\begin{pmatrix} t_x(n) \\ t_y(n) \\ t_z(n) \end{pmatrix} = \begin{pmatrix} \sigma_{xx} & \sigma_{yx} & \sigma_{zx} \\ \sigma_{xy} & \sigma_{yy} & \sigma_{zy} \\ \sigma_{xz} & \sigma_{yz} & \sigma_{zz} \end{pmatrix} \begin{pmatrix} n_x \\ n_y \\ n_z \end{pmatrix}$$

The magnitude of the traction vector normal to the dyke ($\sigma_\perp$) is then given by $(\mathbf{t}\cdot\hat{\mathbf{n}})$.

To determine the probability of a dyke being intruded with the equivalent percentage of opening in unclamped regions as observed, we first calculate a probability function based on the location of dyke opening between 2006 and

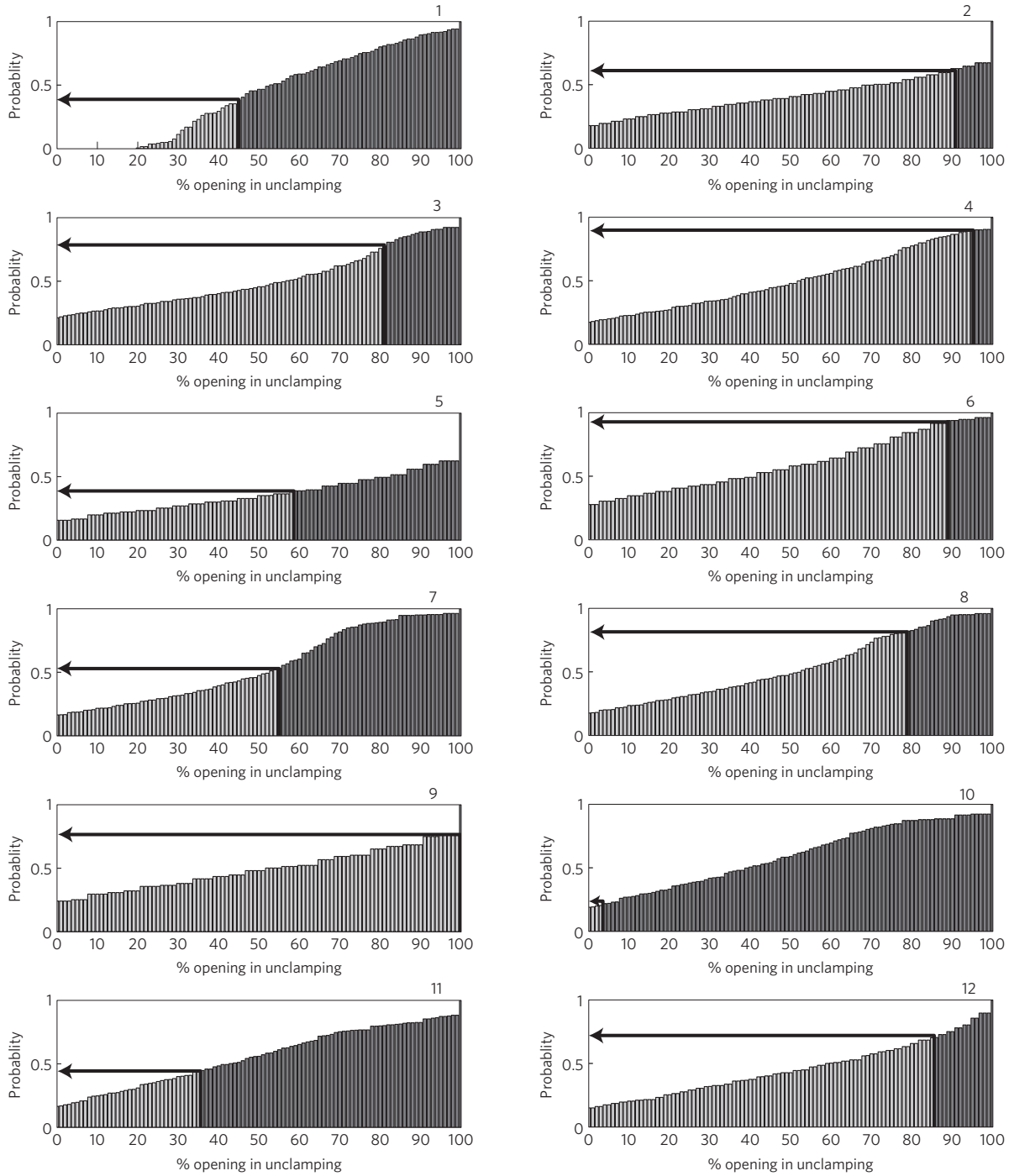

Figure 3 | Cumulative probability histograms calculated for each of the dyke intrusions between June 2006 and July 2009, showing the likelihood of each dyke exceeding a given percentage of opening in regions where tensile stresses were increased by the previous dyke. The black arrow shows the likelihood of the observed dyke having more than the observed amount of dyke opening in unclamped sections of the rift. The area shaded in dark grey highlights the region where the percentage of opening, in unclamped sections of the rift, for the simulated dykes exceeds the observed percentage. In the case of dyke 1 this indicates that there is a 0.6 probability of the intrusion having more than 45% of its opening in an area unclamped by the previous dyke.

2009 (Supplementary Fig. S3). For each along axis and depth position we sum the number of dyke intrusions which have had opening at that location (Supplementary Fig. SM3) and fit a probability function of the form:

$$y = \frac{1}{\sigma\sqrt{2\pi}} \exp^{-\frac{(x-\bar{x})^2}{2\sigma^2}}$$

where y is the frequency, σ is the standard deviation, x is the along axis or depth location and $\bar{x}$ is the mean location. The probability grid is then calculated by multiplying together the two functions for depth and along axis position. Taking the opening models shown in Fig. 2, we reposition each model at every possible location across the modelled dyke plane while keeping the stress change from the previous intrusion fixed. For each of the repositioned dykes we assess the percentage of opening in areas of unclamping and assign a likelihood, corresponding to the probability value generated from the probability function, at the centre of the dyke which is dependent on its position within the model domain. The probability of a dyke having x% of its opening in regions of unclamping then becomes the sum of the likelihoods for all of the repositioned dykes with the same amount of opening in unclamped sections of the rift.

$$P_{\mathrm{tot}}(D_{x\%}) = \sum P_{\mathrm{ind}}(D_{x\%})$$

The cumulative probability function (CDF), plotted in Fig. 3, for each intrusion is then

$$P(D_{<x\%}) = \sum_{0}^{x} P(D_{x\%})$$

The probabilities plotted in each of the histograms in Fig. 3 represent the likelihood, $P(D_{x\%})$, of each dyke having less than x% of its opening in sections of unclamping. For example, the probability of a dyke to have less than 100% of its opening in unclamped sections is always 1. This is because, regardless of its position in the model domain, it will always have less than 100% of its opening in unclamped sections.

Received 31 March 2010; accepted 25 August 2010; published online 26 September 2010; corrected online 1 October 2010

References

1. Reasenberg, P. A. & Simpson, R. W. Response to regional seismicity to the static stress change produced by the Loma Prieta earthquake. *Science* **255,** 1687–1690 (1992).
2. King, G. C. P., Stein, R. S. & Lin, J. Static stress changes and the triggering of earthquakes. *Bull. Seismol. Soc. Am.* **84,** 935–953 (1994.).
3. Harris, R. A. & Simpson, R. W. In the shadow of 1857—the effect of the Great Ft. Tejon earthquake on subsequent earthquakes in southern California. *Geophys. Res. Lett.* **23,** 229–232 (1996).
4. Walter, R. & Amelung, F. Volcano–earthquake interaction at Mauna Loa volcano, Hawaii. *J. Geophys. Res.* **111,** B05204 (2006).
5. Amelung, F., Yun, S. H., Walter, T. R., Segall, P. & Kim, S. W. Stress control of deep rift intrusion at Mauna Loa volcano, Hawaii. *Science* **316,** 1026–1030 (2007).
6. Calais, E. *et al.* Strain accommadation by slow slip and dyking in a youthful continental rift, East Africa. *Nature* **456,** 783–787 (2008).
7. Wright, T. J. *et al.* Magma-maintained rift segmentation at continental rupture in the 2005 Afar dyking episode. *Nature* **442,** 291–294 (2006).
8. Yirgu, G., Ayele, A. & Ayalew, D. Recent seismovolcanic crisis in northern Afar, Ethiopia. *EOS Trans. AGU* **87,** 325–336 (2006).
9. Ayele, A. *et al.* The volcano-seismic crisis in Afar, Ethiopia, starting September 2005. *Earth Planet. Sci. Lett.* **255,** 177–187 (2007).
10. Barisin, I., Leprince, S., Parsons, D. & Wright, T. Surface displacements in the September 2005 Afar rifting event from satellite image matching: Asymmetric uplift and faulting. *Geophys. Res. Lett.* **36,** L07301 (2009).
11. Grandin, R. *et al.* September 2005 Manda Hararo–Dabbahu rifting event, Afar (Ethiopia): Constraints provided by geodetic data. *Geophys. Res. Lett.* **114,** B08404 (2009).
12. Ayele, A. *et al.* September 2005 mega-dike emplacement in the Manda–Harraro nascent oceanic rift (Afar depression). *Geophys. Res. Lett.* **36,** L20306 (2009).
13. Hamling, I. J. *et al.* Geodetic observations of the ongoing Dabbahu rifting episode: New dyke intrusions in 2006 and 2007. *Geophys. J. Int.* **178,** 989–1003 (2009).
14. Hayward, N. J. & Ebinger, C. J. Variations in the along-axis segmentation of the Afar rift system. *Tectonics* **15,** 244–257 (1996).
15. Rowland, J. V. *et al.* Fault growth at a nascent slow-spreading ridge: 2005 Dabbahu rifting episode, Afar. *Geophys. J. Int.* **171,** 1226–1246 (2007).
16. Ebinger, C. *et al.* Capturing magma intrusion and faulting processes during continental rupture: Seismicity of the Dabbahu (Afar) rift. *Geophys. J. Int.* **174,** 1138–1152 (2008).
17. Keir, D. *et al.* Evidence for focused magmatic accretion at segment centres from lateral dike injections captured beneath the Red Sea rift in Afar. *Geology* **37,** 59–62 (2009).
18. Okada, Y. Internal deformation due to shear and tensile faults in a half-space. *Bull. Seismol. Soc. Am.* **82,** 1018–1040 (1992).
19. Cauchy, A. L. Recherches sur l'Équilibre et le Mouvement Intérieur des Corps Solides ou Fluides, Élastiques ou non Élastiques. *Bull. Soc. Philomath.* **2,** 300–304 (1823).
20. Buck, W. R., Einarsson, P. & Brandsdóttir, B. Tectonic stress and magma chamber size as controls on dike propagation: Constrints from the 1975–1984 Krafla rifting episode. *J. Geophys. Res.* **111,** B12404 (2006).
21. Desissa, M. *et al.* A magnetotelluric study of continental lithosphere in the final stages of break-up: Afar, Ethiopia. In IAGA Assembly, Hungary, no. 106-TUE-O1345-1158 in I06 (2009).
22. Stein, R. S. The role of stress transfer in earthquake occurrence. *Nature* **402,** 605–609 (1999).
23. Watanabe, T., Masuyama, T., Nagaoka, K. & Tahara, T. Analog experiments on magma-filled cracks: Competition between external stresses and internal pressure. *Earth Planet. Space* **54,** 1247–1261 (2002).
24. Nooner, S. L. *et al.* Post-rifting relaxation in the Afar region, Ethiopia. *Geophys. Res. Lett.* **36,** L21308 (2009).
25. Rosen, P. A., Hensley, S., Peltzer, G. & Simons, M. Updated repeat orbit interferometry package released. *EOS Trans. AGU* **85,** 47 (2004).
26. Farr, T. & Kobrick, M. Shuttle radar topography mission produces a wealth of data. *EOS Trans. AGU* **81,** 583–585 (2000).
27. Goldstein, R. M. & Werner, C. L. Radar interferogram filtering for geophysical applications. *Geophys. Res. Lett.* **25,** 4035–4038 (1998).
28. Goldstein, R. M., Zebker, H. A. & Werner, C. L. Satellite radar interferometry: Two-dimensional phase unwrapping. *Radio Sci.* **23,** 713–720 (1988).
29. Okada, Y. Surface deformation due to shear and tensile faults in a half-space. *Bull. Seismol. Soc. Am.* **75,** 1135–1154 (1985).
30. Wright, T. J., Lu, Z. & Wicks, C. Constraining the slip distribution and fault geometry of the M_W 7.9, 3 November 2002, Denali fault earthquake with interferometric synthetic aperture radar and global positioning system data. *Bull. Seismol. Soc. Am.* **94,** 175–189 (2004).

Acknowledgements

We would like to thank the Geophysical Observatory of Addis Ababa University, the Afar Regional government and the Ethiopian Ministries of Capacity Building, and of Mines and Energy for their help and support. Thanks to J. Cann, G. Houseman, J. Neuberg and R. Buck for discussions and to C. Ebinger for help with GPS data acquisition and funding support. Our work is supported by NERC grants NE/D008611/1, NE/D01039X/1 and NE/E007414/1, NSF grants EAR-0635789 and EAR-0613651, a NERC-COMET studentship to I.J.H., an Exxon-Mobil fellowship to L.B. and a Royal Society University Research Fellowship to T.J.W. Radar data is from the European Space Agency under project C1P-3435.

Author contributions

I.J.H. and T.J.W. planned and processed the InSAR data. E.C., L.B. and E.L. collected and processed GPS data. I.J.H. carried out the elastic modelling and wrote the paper with contributions from all the co-authors.

Additional information

The authors declare no competing financial interests. Supplementary information accompanies this paper on www.nature.com/naturegeoscience. Reprints and permissions information is available online at http://npg.nature.com/reprintsandpermissions. Correspondence and requests for materials should be addressed to I.J.H.

ERRATUM

Stress transfer between thirteen successive dyke intrusions in Ethiopia

Ian J. Hamling, Tim J. Wright, Eric Calais, Laura Bennati and Elias Lewi

Nature Geoscience **3,** 713–717 (2010); published online: 26 September 2010; corrected after print: 1 October 2010.

In the version of this Letter originally published, the positions of several of the outlines of dyke openings in Figure 2 were incorrect and should have been as shown here. These errors have now been corrected in the HTML and PDF versions of the text.